HHS Public Access

Author manuscript

J Immunol. Author manuscript; available in PMC 2023 March 15.

Published in final edited form as:

J Immunol. 2022 March 15; 208(6): 1456–1466. doi:10.4049/jimmunol.2100741.

TFAM-dependent mitochondrial metabolism is required for alveolar macrophage maintenance and homeostasis

Xiaochen Gao[1,2], **Bibo Zhu**[1,2], **Yue Wu**[1,2], **Chaofan Li**[1,2], **Xian Zhou**[1,3], **Jinyi Tang**[1,2], **Jie Sun**[1,2,4,5,6]

[1]Department of Immunology, Mayo Clinic, Rochester, MN 55905, USA.

[2]Division of Pulmonary and Critical Medicine, Department of Medicine, Mayo Clinic, Rochester, MN 55905, USA.

[3]Division of Rheumatology, Department of Medicine, Mayo Clinic College of Medicine and Science, Mayo Clinic, Rochester, MN 55905, USA.

[4]Department of Physiology and Biomedical Engineering, Mayo Clinic, Rochester, MN 55905, USA.

[5]Carter Immunology Center, University of Virginia, Charlottesville, VA 22908, USA

[6]Division of Infectious Disease and International Health, Department of Medicine, University of Virginia, Charlottesville, VA 22908, USA.

Abstract

Alveolar macrophages (AMs) are major lung tissue-resident macrophages capable of proliferating and self-renewal *in situ*. AMs are vital in pulmonary anti-microbial immunity and surfactant clearance. The mechanisms regulating AM compartment formation and maintenance remain to be fully elucidated currently. Here we have explored the roles of mitochondrial transcription factor A (TFAM)-mediated mitochondrial fitness and metabolism in regulating AM formation and function. We found that TFAM deficiency in mice resulted in significantly reduced AM numbers and impaired AM maturation *in vivo*. TFAM deficiency was not required for the generation of AM precursors (Pre-AMs) nor the differentiation of Pre-AMs into AMs, but was critical for the maintenance of AM compartment. Mechanistically, TFAM-deficiency diminished gene programs associated with AM proliferation and self-renewal, and promoted the expression of inflammatory genes in AMs. We further showed that TFAM-mediated AM compartment impairment resulted in defective clearance of cellular debris and surfactant in the lung, and increased the host susceptibility to severe influenza virus infection. Finally, we found that influenza virus infection in AMs led to impaired TFAM expression and diminished mitochondrial fitness and metabolism. Thus, our data have established the critical function of TFAM-mediated mitochondrial metabolism in AM maintenance and function.

*Corresponding author, js6re@virginia.edu.

Introduction

Alveolar macrophages (AMs) are the main tissue-resident macrophages in the respiratory tract. AMs mainly derive from yoke sac precursors of fetal monocytes, which populate the alveolar space in the first week after birth (1, 2). During their differentiation and maturation, AM undergo profound phenotypical changes, which are characterized by increased expression of CD11c, Siglec-F, F4/80 and CD64, and concomitant down-regulation of CD11b (3, 4). After their development, AMs can persist independently of adult bone marrow and monocyte contribution via self-renew *in situ*. AMs are critical in the maintenance of lung homeostasis, surfactant clearance, anti-microbial immunity and tissue repair in the respiratory tract (5). The absence of AMs or impaired AM function can cause pulmonary alveolar proteinosis, which is a rare disease due to alveolar accumulation of surfactant and respiratory insufficiency (6, 7). AMs are also important for the protection against a variety of respiratory bacterial, fungal and viral infections including influenza virus infection (5). AMs can phagocytize free virus and virus-infected cells, produce anti-viral cytokines, protect alveolar type I cells, clear cellular debris and repair damaged lungs following influenza virus infection (8–13).

The granulocyte-macrophage colony-stimulating factor (GM-CSF) and transforming growth factor β (TGF-β) are the two critical cytokines required for the differentiation and maintenance of AMs. The transcription factor PPARγ, induced by GM-CSF and TGF-β, is vital for AM differentiation and maintenance (1, 11, 14). Bach2, Bhlhe40 and Bhlhe41, Hematopoietic protein-1 (Hem-1), mTORC1, Phosphoinositide Kinase, FYVE-Type Zinc Finger (PIKfyve), Lkb1 and L-plastin etc were also shown to be important in AM development, maintenance and/or function (15–20). Interestingly, both PPARγ and Bach2-deficiency profoundly altered AM lipid metabolic responses (11, 15). Suggesting that functional cellular metabolic state is likely required for AM homeostasis and/or function. In support of this idea, mTORC1-mediated glucose metabolism has been linked to AM maintenance and proliferation *in vivo* (20). Nevertheless, the exact function of individual metabolic pathways on AM formation and/or function remain to be fully elucidated *in vivo*.

The mitochondria are the central hub of cellular metabolic responses, which are required for ATP generation, macromolecule biosynthesis, calcium homeostasis, redox balance and cellular epigenetic programming (21–24). The mitochondrial transcription factor A (TFAM) is a nuclear-encoded transcription factor that plays a critical role in mitochondrial (mt) DNA replication, metabolism and stability (25). As such, TFAM deficiency causes severe mtDNA depletion, mitochondria damage and non-functional oxidative phosphorylation (OXPHOS) (26). Furthermore, TFAM has been shown to play a crucial role in mtDNA stress-mediated inflammatory responses (27, 28). The roles of mitochondrial metabolism and TFAM function in regulating AM development, maintenance and/or proliferation are unknown currently. We have recently shown that AM self-renewal and inflammatory responses were uncoupled by mitochondrial metabolism (29). As such, the inhibition of mitochondrial respiratory complex function resulted in diminished AM proliferation *in vitro* and *in vivo* (29). Given the roles of TFAM in maintaining cellular mitochondrial metabolism and suppressing inflammatory responses (27, 28), we hypothesized that TFAM-dependent mitochondrial oxidative metabolism is likely required for AM self-renewal and/or function.

In this report, we showed that TFAM deficiency caused impaired AM mitochondrial fitness, altered metabolism and defective lipid catabolic responses, leading to diminished AM quantity and altered AM phenotypes. We demonstrated that TFAM deficiency did not impair AM differentiation from their precursors, but caused reduced AM maintenance. RNA-seq experiment revealed that TFAM deficiency caused impaired AM self-renewal capability. We showed that TFAM deficiency in AMs caused impaired clearance of respiratory debris, surfactant and enhanced susceptibility to severe influenza virus infection. Finally, we found that influenza infection resulted in disruption of TFAM-mediated mitochondrial fitness and metabolism in AMs.

Materials and methods

Mouse and virus

C57BL/6, CD45.1$^+$, CD11c-cre, Ubc-creERT2, *Tfam*$^{fl/fl}$ mice were purchased from the Jackson Laboratory. *CD11c*^{cre}*Tfam*$^{fl/fl}$ or *CD11c*^{cre}*Tfam*$^{fl/+}$ mice were generated by crossing *Tfam*$^{fl/fl}$ mice with CD11c-cre mice (30). *Ubc*^{creER}*Tfam*$^{fl/fl}$ mice were generated by crossing *Tfam*$^{fl/fl}$ mice to mice expressing a cre-ERT2 fusion gene under the control of the human ubiquitin C (Ubc) promoter (31). All mice were maintained in a specific pathogen-free environment at the Mayo Clinic animal facility. For Influenza virus infection, Influenza A/PR8/34 strain was diluted in FBS-free DMEM media (Gibco) on ice, and inoculated in anesthetized mice by intranasal route (i.n.) as described before (32).

Bronchoalveolar lavage (BAL) fluid

After mice were sacrificed, BAL fluid was obtained by flushing the airway three times with a single inoculum of 600 μL sterile cold PBS via a trachea incision. Cells in the 600 μL of BAL fluid were centrifuged at 1600 rpm at 4 °°C for 5 min, and supernatants were collected for the determination of turbidity, protein concentration and cytokines/chemokines levels as indicated in the text. Cell pellets were resuspended in 1 mL PBS and used for further flow cytometry analysis.

Lung cell suspension preparation

Lungs were collected from sacrificed mice. Lung tissues were cut into small pieces by scissors, and digested with Collagenase Type 2 (183 Unit/mL, Worthington Biochemical) for 30 min at 37 °°C. The single cell suspension was passed through a 70 μm cell strainer (Falcon) within a 50 mL falcon tube. Cells were pelleted at 1600 rpm at 4 °°C for 5 min, and the pellet was suspended after lysing red blood cells (RBCs) with ACK lysis buffer (0.15 M NH_4Cl, 1 mM $KHCO_3$, 0.1 mM Na_2EDTA, pH 7.2). After centrifugation at 1600 rpm at 4 °°C for 5 min, the cell pellet was suspended in cold flow cytometry buffer for flow cytometry analysis.

AM culture and treatment *in vitro*

AMs were obtained from BAL as described previously (29). Briefly, mice were euthanized, the skin and muscles were removed on trachea, a small incision was made below larynx. This incision was inserted by 1 mL pipette toward to lungs. Alveolar lavages were performed with multiple 1 ml flush of the lungs with 2 mM EDTA

(ethylenediaminetetraacetic acid) in 2% FBS (fetal bovine serum)/PBS (phosphate buffered saline). Pooled BAL washes were centrifuged at 1600 rpm at 4 °°C for 5 min to pellet cells. AMs were purified by adherence to culture plate for 2 h in complete medium (RPMI1640, 10% FBS, 1% Pen/Strep/glutamate, Thermo Fisher) at 37 °°C and 5% CO_2. The non-adherent cells were washed off with warm PBS.

For AM infection *in vitro*, seeded cells were initially incubated with 10 multiplicity of infection (MOI) of influenza PR8 virus in PBS for 15 minutes on ice. Then, the cells were cultured in at 37 °°C and 5% CO_2 for 1 hour. Virus was subsequently washed out with warm PBS for twice. The cells were further cultured in warm complete medium containing 10 ng/mL GM-CSF for additional 24 h at 37 °°C and 5% CO_2. Cells were analyzed by quantitative RT-PCR, Western blot, Transmission electron microscopy.

To assess AM proliferation, AMs were first cultured overnight in complete medium without GM-CSF. Then, AMs were cultured in complete medium supplemented with 10 ng/mL recombinant murine granulocyte macrophage colony-stimulating factor (rGM-CSF, Biolegend) for 24 h. The cells were digested by 0.25 % Trypsin-EDTA solution and collected for flow cytometric staining including staining cell surface markers and intracellular staining of Ki-67.

BM neutrophil and monocyte isolation

Bone marrow cells were collected from tibias and femurs by flushing with cold PBS through a 25 gauge needle. The single cell suspension was passed through a 70 μm cell strainer in a 50 mL falcon tube. Cells were pelleted at 1600 rpm for 5 min, and the pellet was suspended in ACK lysis buffer (0.15 M NH4Cl, 1 mM KHCO3, 0.1 mM Na2EDTA, pH 7.2) at room temperature for 5 min. After centrifugation at 1600 rpm for 5 min, the cell pellet was suspended in 90 μL of cold MACS buffer for per 10^7 total cells. According to the protocol for Anti-Ly6G Microbeads (Miltenyi Biotec), added 10 μL of Anti-Ly6G beads and incubated for 10 min in 4 °°C, and then washed by MACS buffer at 1600 rpm for 5 min. Cells were resuspended and applied onto column, column was washed and then collected $ly6G^+$ cells (BM-neutrophils). $ly6G^-$ cells added Anti-CD11b Microbeads (Miltenyi Biotec), similarly collected $ly6G^-CD11b^+$ cells (BM-monocytes).

Transmission electron microscopy

In vitro cultured AMs or sorted AMs as indicated in the text were fixed in 2% paraformaldehyde and 2.5% glutaraldehyde in 0.1 M sodium cacodylate. Following fixation, cells were embedded and sliced for transmission electron microscopy. The Grids were imaged with a JEM 1400 transmission electron microscope (JEOL). Mitochondrial morphology was scored as normal or abnormal. Structurally abnormal mitochondria were defined operationally as those with loss of cristae, decreased electron density of the matrix, loss of integrity of mitochondrial membrane and/or the formation of autophagosomes structures as reported before (33). The number of damaged mitochondria and total mitochondria per cell was quantified.

BAL fluid turbidity and protein assay

The turbidity of BAL fluid was assessed with the optical density at a wavelength of 590 nm (OD590) by spectrophotometry. Total protein of BAL fluid was determined by BCA protein assay kit (Thermo Scientific) according to the manufacture manual. 50 μL of each BAL sample was used. VERSAmax microplate reader (Molecular Devices) was used for colorimetric quantification and analysis at OD 562 nm wavelength.

Multiplex cytokine/chemokine quantification

Cytokine and chemokine levels in BAL fluid were shipped in dry ice to Eve Technologies and measured with Mouse Cytokine Array/Chemokine Assay 31-Plex (MD31).

Seahorse analysis

Real-time oxygen consumption rate (OCR) and extracellular acidification rate (ECAR) of AMs were measured with a Seahorse XFp Analyzers as described previously (Seahorse Bioscience) (23). AMs (10^5) were seeded into each well of Seahorse XFp Cell Culture Miniplates for overnight at 37 °C and 5% CO_2. On the following day, the cells were washed twice and incubated at 37 °C for 1h in the absence of CO_2 in unbuffered assay medium (pH=7.4, Agilent Technologies) with 10 mM glucose for mitochondria stress test. OCR was measured under basal conditions and after the addition of the following compounds: 1 μM oligomycin (ATP synthase inhibitor), 1.5 μM FCCP (carbonyl cyanide-4-(trifluoromethoxy) phenylhydrazone) and 0.5 μM rotenone + 0.5 μM antimycin (Complex I and III inhibitor). ECAR was measured with the addition of following compounds: 10 mM glucose, 1 μM oligomycin and 50 mM 2-DG (2-deoxy-D-glucose). All compounds obtained from Sigma. Data were analyzed with Wave Desktop software version 2.6 (Agilent Technologies).

Mitochondrial membrane potential analysis

BAL cells were harvested in flow cytometry staining buffer (FACS buffer; 2mM EDTA, 0.05% sodium azide and 2% FBS in PBS) and stained with surface markers (CD11c, CD11b and Siglec F). The cells were washed twice with PBS, and then resuspended in 100 μl PBS containing 500 nM MitoTracker ™ Green FM (Thermo Fisher). Cells were stained for 45 min at 37 °C according to the manufacturer's protocol. Then cells were washed twice in PBS and analyzed by flow cytometry.

BODIPY assay

BAL cells were harvested in FACS buffer and stained with surface markers. According to the protocol of fluorescent BODIPY™ 493/503 (4, 4-Difluoro-1, 3, 5, 7, 8-Pentamethyl-4-Bora-3a, 4a-Diaza-s-Indacene) (Thermo Fisher), the cells were washed twice in PBS, and then resuspended in media containing fluorescent BODIPY™ 493/503 for 10 min at room temperature. Cells were washed three times in FACS buffer and analyzed by flow cytometry.

Flow cytometry

Cell staining was performed with the appropriate antibody cocktail in FACS buffer. The cell subsets were identified based on following cell surface markers: AM ($CD11c^+$ Siglec F^+ $CD11b^{low}$ $CD64^+$ $MerTK^+$), immature AM ($CD11c^+$ Siglec F^{low} $CD11b^{low}$ $CD64^+$

MerTK^{+}), Pre-AM (CD45^{+} CD11c^{+} Siglec F^{-} CD11b^{int} F4/80^{+} Ly6C^{-}), Neutrophils (CD11b^{+} Ly6G^{+}), Ly6C^{hi} Monocytes (Ly6G^{-} Siglec F^{-} CD11b^{+} Ly6C^{hi}), Dendritic cells (CD11c^{+} MHCII^{+}). Fluorescence-conjugated antibodies CD11b (M1/70), CD11c (N418), CD64 (X54–5/7.1), MerTK (2B10C42), F4/80 (BM8), Ly6G (1A8), Ly6C (HK1.4), MHCII (M5/114.15.2), CD45 (30-F11), Ki67 (SolA15) were purchased from Biolegend, and Siglec F (E50–2440) was from BD Biosciences, and NP366 tetramer^{+} cells (CD8^{+} NP366-tet^{+}), PA224 tetramer^{+} cells (CD8^{+} PA224-tet^{+}) (NIH Tetramer Facility). For Ki67 staining, cell suspensions were stained for surface marker at 4 °°C for 30 min. Cells were washed twice with FACS buffer, prior to fixation and permeabilization with the Foxp3 transcription factor staining buffer set (eBioscience) for 1h at room temperature (RT) in the dark. Cells were washed twice with perm wash buffer (eBioscience), and stained with Abs against Ki67 (eBioscience) and control immunoglobulin (Biolegend) in perm wash buffer for at least 30 min at RT in the dark. Cells were subsequently washed twice with perm wash buffer before samples were processed with flow cytometer. Samples were collected on FACS Attune NXT flow cytometer (Life technologies) and analyzed using FlowJo software (Tree star).

Lung histopathology

Mice were perfused with PBS (10 mL) via the right ventricle following euthanasia. Paraformaldehyde (PF, 10%) was then gently instilled into the lung and left inflated for 1 minute before excising and moving lobe to 10% PF. Samples were shipped to Mayo Clinic Histology Core Lab (Scottsdale, AZ) where they were embedded in paraffin and 5 μm sections were cut for Hematoxylin and eosin stain. To quantify percent of inflamed or disrupted alveolar area, slides were scanned through the Aperio whole slide scanning system (Leica) and exported to image files. Computer-based image analysis was performed using the Image J software (NIH, Bethesda, MD, USA). We first determined the total lung area by converting the image into gray scale, followed by red highlighting through the adjustment of the threshold. For determination of the inflamed and disrupted area, color images were split into single channels. We then used the green channel, highlighted the inflamed areas in red by adjusting the threshold and measured the areas based on pixel. The percentages of disrupted and inflamed lung areas were calculated based on the ratio of highlighted disrupted areas to the total lung area in each lung section.

Tamoxifen treatment

To induce gene recombination in *Ubc*^{creER}*Tfam*$^{fl/fl}$ mice, tamoxifen ((E/Z)-4-hyroxy Tamoxifen, Cayman) was dissolved in 0.5 mL of ethanol and 9.5 mL of warm sunflower oil (Sigma-Aldrich). And then the suspension administered at 2 mg/mouse at a concentration of 20 mg/mL via intraperitoneal injection (i.p.) for five consecutive days.

Bone marrow chimeras

To generate mixed bone marrow chimeric mice, WT recipient mice were lethally irradiated (1000 Rads for females or 1100 Rads for males), and then i.v. injected an equal mix of ~ 6 million bone marrow cells from WT CD45.1 bone marrow and *Tfam*$^{fl/fl}$ or *Ubc*^{creER}*Tfam*$^{fl/fl}$ CD45.2 donors (mixed at 1:1 ratio). Following 7 weeks of reconstitution, recipient mice were daily administered 2 mg/mouse of tamoxifen via intraperitoneal route

for five consecutive days. BAL and lung samples were obtained at indicated time in the text post injection.

RNA-sequencing and analysis

Total RNA of AMs was extracted using RNeasy Plus Mini Kit (Qiagen) following the manufacture's protocol. Two pools per genotype were used for RNA-seq. After quality control, high quality (Agilent Bioanalyzer RIN >7.0) total RNA was used to generate the RNA sequencing library. cDNA synthesis, end-repair, A-base addition, and ligation of the Illumina indexed adapters were performed according to the TruSeq RNA Sample Prep Kit v2 (Illumina, San Diego, CA). The concentration and size distribution of the completed libraries was determined using an Agilent Bioanalyzer DNA 1000 chip (Santa Clara, CA) and Qubit fluorometry (Invitrogen, Carlsbad, CA). Paired-end libraries were sequenced on an Illumina HiSeq 4000 following Illumina's standard protocol using the Illumina cBot and HiSeq 3000/4000 PE Cluster Kit. Base-calling was performed using Illumina's RTA software (version 2.5.2). Paired-end RNA-seq reads were aligned to the mouse reference genome (GRCm38/mm10) using Bowtie (v2.3.4). Pre- and post-alignment quality controls, gene level raw read count and normalized read count (i.e. FPKM) were performed using RSeQC package (v2.3.6) with NCBI mouse RefSeq gene model. For functional analysis, GSEA was performed to identify enriched gene sets using the hallmark collection of the Molecular Signatures Database (MSigDB), having up- and down-regulated genes, and using a weighted enrichment statistic and a $\log_2$ ratio metric for ranking genes. Data was submitted to GEO repository (GSE188279, https://www.ncbi.nlm.nih.gov/geo/query/acc.cgi?acc=GSE188279).

Statistical analysis

Unpaired two-tailed Student's t-test (two group comparison), one-way ANOVA (multiple group comparison), Multiple t-tests (weight loss and Multiplex studies) or Log-rank (Mantel-Cox) test (survival data) were used to determine statistical significance by GraphPad Prism software. A P value < 0.05 was considered significant (*, $p < 0.05$; **, $p < 0.01$; ***, $p < 0.001$).

Results

TFAM deficiency resulted in diminished AM numbers and metabolic fitness

To investigate the role of TFAM in AM development and/or function, we crossed *Tfam* floxed mice to transgenic mice that express Cre recombinase under CD11c (*Itgax*) promoter (34). CD11c is highly expressed in AM precursors, mature AMs and dendritic cells (DCs) (1, 30). Previously, we have shown that CD11c-Cre mediates high efficiency of gene recombination of loxP-flanked DNA in DCs and AMs, but very moderately in other immune cell types in the respiratory tract (30). Indeed, we confirmed that $CD11c^{cre}Tfam^{fl/fl}$ mice had impaired TFAM expression in AM compartment, moderately diminished expression in whole lung cells (potentially due to diminished TFAM expression in AMs and lung DCs), but not in neutrophils or monocytes isolated from the bone marrow (BM) compartment (Supplemental Fig. 1A).

At the adult age (7–8 weeks-old), percentages and cell numbers of mature AM (MERTK^{+} CD64^{+} CD11c^{hi} Siglec F^{hi}) (35) were significantly decreased in the BAL and lungs of *CD11c^{cre}Tfam$^{fl/fl}$* mice compared to those of *Tfam$^{fl/fl}$* or CD11c-cre *Tfam$^{fl/+}$* (het) mice (Fig. 1A, 1B, gating strategy shown in Supplemental Fig. 1B) (29). In contrast, immature AM (MERTK^{+} CD64^{+} CD11c^{hi} Siglec F^{low}) (36, 37) were increased following TFAM deficiency. The levels of lung interstitial macrophages (IM, MERTK^{+} CD64^{+} Siglec F^{-}) (35) were moderately elevated in *CD11c^{cre}Tfam$^{fl/fl}$* mice comparable those of WT or Het mice (Fig. 1B). There were increased levels of DCs and neutrophils in the BAL of *CD11c^{cre}Tfam$^{fl/fl}$* mice, but the levels of these cell types in the lungs were comparable across WT, Het and *CD11c^{cre}Tfam$^{fl/fl}$* mice (Supplemental Fig. 1C, 1D). After birth, mature AM highly expressed CD11c and Siglec F and but low CD11b (1, 38). In consistent with the increased levels of immature AM presence, BAL AM in *CD11c^{cre}Tfam$^{fl/fl}$* mice expressed higher levels of CD11b than those of WT or Het mice (Fig. 1C).

TFAM expression is crucial for mitochondrial fitness and function (26). We therefore examined whether TFAM deficiency affected AM metabolism. To this end, we measured mitochondrial oxidative phosphorylation and glycolysis of BAL AMs from *Tfam$^{fl/fl}$* or *CD11c^{cre}Tfam$^{fl/fl}$* mice. We found that basal oxygen consumption rate (basal OCR) and maximal mitochondrial respiratory capacity (max. respiration) were decreased in AMs following TFAM deficiency (Fig. 1D, 1E). Furthermore, extracellular acidification rate (ECAR) of AMs were also decreased (Fig. 1F). These data suggest that TFAM deficiency impairs AM metabolic fitness. Consistent with decreased OCR, TFAM-deficient AMs had decreased mitochondrial mass as measured by MitoTracker staining (Fig. 1G). We then evaluated mitochondrial morphology of BAL AMs from *Tfam$^{fl/fl}$* or *CD11c^{cre}Tfam$^{fl/fl}$* mice by transmission electron microscopy (TEM) (Fig. 1H). TFAM-deficient AMs had decreased overall mitochondrial numbers and increased percentages of abnormal mitochondria (mitochondrial swelling and loss of cristae) (Fig. 1H). Together, these data suggest that TFAM deficiency impairs mitochondrial fitness and metabolism. Mitochondria are essential for lipid catabolism in cells. Consistently, we found that TFAM-deficient AMs had increased lipid content in AMs and enlarged lipid droplets within the cytoplasm (Fig. 1I, 1J).

TFAM is not essential for early AM differentiation

We next sought to track the kinetics of AM responses following TFAM deficiency. To this end, we first examined AM numbers and phenotypes at the juvenile stage (week 3–4 postnatally). We found that the percentages and numbers of mature BAL AMs were significantly diminished in *CD11c^{cre}Tfam$^{fl/fl}$* mice compared to those of *Tfam$^{fl/fl}$* mice, albeit to a lower extent as in the adult age (7–8 weeks) (Fig. 2A, Supplemental Fig. 2A). Accompanied with this, immature AMs were significantly elevated in the lung of *CD11c^{cre}Tfam$^{fl/fl}$* mice (Supplemental Fig. 2B). Lung neutrophils, DCs and Ly6C^{hi} monocytes were at similar levels between *CD11c^{cre}Tfam$^{fl/fl}$* mice and *Tfam$^{fl/fl}$* mice at the 3–4 weeks age (Supplemental Fig. 2C, 2D). Similarly, TFAM-deficient AMs had decreased mitochondrial oxidative phosphorylation as measured by OCR (Fig. 2B, 2C).

AMs are mainly developed from fetal monocytes through a pre-AM stage in the first week of birth (1). To explore the function TFAM in early AM differentiation, we examined the

monocyte and macrophage populations in the lung at day 3 post birth (PND3). We found that overall lung myeloid cells ($CD11b^+$ $F4/80^+$) were comparable between $Tfam^{fl/fl}$ and $CD11c^{cre}Tfam^{fl/fl}$ mice at PND3 (Fig. 2D). Using the gating strategy reported before (1), we found that lung AMs ($CD11c^+$ Siglec F^+ $Ly6C^-$ $F4/80^+$), pre-AM ($CD11c^{int}$, $Ly6C^-F4–80^+$Siglec F^-), monocytes ($CD11c^-$ $Ly6C^+$ Siglec F^- $F4/80^-$) and fetal macrophages ($CD11c^-$ $Ly6C^+$ Siglec F^- $F4/80^+$) were comparable between $Tfam^{fl/fl}$ and $CD11c^{cre}Tfam^{fl/fl}$ mice at PND3 (Fig. 2D, 2E). Similar results were observed at PND7 (Fig. 2F). These data suggest that TFAM deficiency likely does not affect the formation of pre-AM population and the differentiation of Pre-AM into AM lineage.

TFAM regulates AM maintenance

Our kinetic analysis suggests that TFAM may not be needed for the initial formation of AM compartment, but is likely required for the maintenance of AM population. However, CD11c-Cre transgenic mice constitutively express Cre recombinase under CD11c promoter, which likely causes TFAM deficiency in AM precursors (37). We therefore can not determine whether TFAM is required for AM maintenance using $CD11c^{cre}Tfam^{fl/fl}$ mice. To address the function of TFAM in AMs following their development, we crossed $Tfam^{fl/fl}$ mice to Ubc-Cre ERT2 transgenic mice (31), in which all cells express a CreERT2 recombinase under human ubiquitin C promoter, to generate Ubc^{creER} $Tfam^{fl/fl}$ mice. The presence of tamoxifen in Ubc^{creER} $Tfam^{fl/fl}$ mice is expected to result in the translocation of the recombinase into the nucleus, where it can recombine loxP-flanked exon 6–7 of *Tfam* to acutely deplete TFAM expression. We injected adult $Tfam^{fl/fl}$ or Ubc^{creER} $Tfam^{fl/fl}$ mice with tamoxifen. We first confirmed the diminished TFAM levels in AMs and other cell types following tamoxifen injection (Supplemental Fig. 3A).

3–4 weeks following injection, we examined BAL AM responses. Acute depletion of TFAM resulted in decreased mature AM numbers in the BAL (Fig. 3A), suggesting that TFAM is likely needed for AM maintenance. Tamoxifen injection in Ubc^{creER} $Tfam^{fl/fl}$ mice will deplete TFAM protein ubiquitously. To determine whether intrinsic TFAM expression in AMs is required for their maintenance, we generated a mixed bone marrow (BM) chimera mice, in which we transplant 1:1 mixed WT ($CD45.1^+$) and Ubc^{creER} $Tfam^{fl/fl}$ ($CD45.2^+$) BM cells into lethally irradiated $CD45.1^+/CD45.2^+$ WT mice. After 7 weeks reconstitution, we injected tamoxifen into the BM chimeric mice and followed AM maintenance (Fig. 3B). At two days following last tamoxifen injection, $CD45.2^+$ TFAM-deficient AMs moderately out-numbered WT $CD45.1^+$ AMs in both BAL and the lung compartment, suggesting that TFAM deficiency did not result in the acute loss of AMs at this early time points (Fig. 3C). However, at 7 weeks after tamoxifen injection, we found that WT $CD45.1^+$ AMs significantly out-numbered TFAM-deficient $CD45.2^+$ AMs in both BAL and the lung compartment, indicating that intrinsic TFAM function is required for AM maintenance (Fig. 3C). In consistency, we found that TFAM deficiency diminished Siglec F but increased CD11b expression in AMs (Supplemental Fig. 3B, 3C), suggesting that TFAM expression may be required for maintaining the mature AM phenotype. In contrast, TFAM deficiency did not dramatically impair the maintenance of neutrophils, DCs, IM and $Ly6C^{hi}$ monocytes populations (Fig. 3D).

TFAM modulates AM self-renewal and inflammatory responses

To begin to understand the underlying mechanisms by which TFAM modulates AM maintenance, we preformed bulk RNA sequencing of BAL AMs from *Tfam*$^{fl/fl}$ or *CD11c*^{cre}*Tfam*$^{fl/fl}$ (KO) mice at the age of 3–4 and 7–8 weeks. The transcriptional profiles of WT AMs and TFAM-deficient AMs were marked different at both time points (Fig. 4A, 4B). Gene set enrichment analysis (GSEA) of hallmark gene sets found that TFAM deficiency increased the expression of hypoxia, adipogenesis and interferon (IFN) gamma and alpha-responsive genes, but decreased expression of NF-κB, cholesterol, G2M checkpoint and MTORC1 signaling (Fig. 4C). Additionally, stem cell-associated genes, which was indicated in AM proliferation and self-renewal (Fig. 4D) (29), were significantly downregulated in TFAM-deficient AMs. These data suggest that TFAM deficiency may impair AM proliferation and self-renewal capability. To test this idea, we measured Ki67-expression in AMs *ex vivo* from *Tfam*$^{fl/fl}$, CD11c-cre *Tfam*$^{fl/+}$ (het) or *CD11c*^{cre}*Tfam*$^{fl/fl}$ (KO) mice at 3–4 weeks of age. TFAM-deficiency significantly was down-regulated Ki67 expression *in vivo* (Fig. 4E). Furthermore, TFAM-deficiency diminished Ki67 expression in AMs after *in vitro* culture with GM-CSF (Fig. 4F), a major AM growth factor (1, 39). Together these data suggest that TFAM-deficiency impairs AM proliferation and self-renewal, thereby diminishing AM maintenance *in vivo*. GSEA analysis further revealed that TFAM-deficiency caused significant up-regulation of inflammation-associated genes at 7–8 weeks age (Fig. 4G, 4H). Together these transcriptional analyses revealed that TFAM is important in regulating AM proliferation and immune homeostasis.

TFAM deficiency leads to altered alveolar homeostasis and impaired antiviral responses

AMs are critical in clearing debris in the alveolar space and in surfactant homeostasis (40, 41). Consistent with the greatly diminished mature AM numbers in *CD11c*^{cre}*Tfam*$^{fl/fl}$ mice, BAL from *CD11c*^{cre}*Tfam*$^{fl/fl}$ mice contained significantly elevated levels of dead cells or cellular debris than those of *Tfam*$^{fl/fl}$ mice (Fig. 5A). Furthermore, supernatant of BAL from *CD11c*^{cre}*Tfam*$^{fl/fl}$ mice exhibited “milky” appearance and had elevated absorbance at OD590 (Fig. 5B, 5C), suggesting that *CD11c*^{cre}*Tfam*$^{fl/fl}$ mice had impaired clearance of surfactant proteins.

AMs are critical for host anti-microbial responses and AM deficiency or functional impairment can lead to increased susceptibility to severe influenza virus infection (8–13). To this end, we infected adult *Tfam*$^{fl/fl}$ or *CD11c*^{cre}*Tfam*$^{fl/fl}$ mice with influenza A PR8 strain and followed host morbidity and mortality after infection. We found that *CD11c*^{cre}*Tfam*$^{fl/fl}$ lost significant more weight and were succumbed to infection by 10 days post infection compared to WT mice (Fig. 5D, 5E), which were consistent with the critical function of AMs in anti-viral immunity and the maintenance of lung homeostasis during influenza infection (42, 43). And BAL total cells, neutrophils, Ly6C^{hi} monocytes and DCs were elevated in *CD11c*^{cre}*Tfam*$^{fl/fl}$ mice at day 4 post infection (Fig. 5F), Importantly, compared to *Tfam*$^{fl/fl}$ mice, *CD11c*^{cre}*Tfam*$^{fl/fl}$ mice showed similar levels of DCs, total and antigen-specific D^{b} NP$_{366–374}$ and D^{b} PA$_{224–233}$ CD8^{+} T cells in the draining LN and the lung at day 5 post infection (44) (Supplemental Fig. 4A, 4B), suggesting that *Tfam* deficiency in CD11c^{+} cells may not change the quantity and function of DCs. Furthermore, *CD11c*^{cre}*Tfam*$^{fl/fl}$ mice exhibited increased tissue inflammation and pathology compared to

Tfam$^{fl/fl}$ mice (Fig. 5G, Supplemental Fig. 4C). Additionally, there was greatly increased pulmonary inflammation in *CD11c*^{cre}*Tfam*$^{fl/fl}$ mice as evidenced by their elevated airway proinflammatory cytokine and chemokine levels compared to those of *Tfam*$^{fl/fl}$ mice. Taken together, these data suggest that TFAM-mediated AM maintenance is critical for preventing severe host inflammation and diseases following influenza virus infection.

Influenza infection leads to decreased TFAM expression and diminished mitochondrial fitness

Proper AM homeostasis is critical for host protective responses following influenza virus infection. Notably, influenza virus can directly infect AMs to impair its function and/or prime inflammatory responses (13, 45). Given the important roles of TFAM-mediated mitochondrial metabolism in regulating AM homeostasis and function, we examined whether influenza infection could decrease TFAM expression in WT AMs. Influenza virus infection caused diminished TFAM protein levels in mouse AMs (Fig. 6A). Consistently, influenza virus infection resulted in increased accumulation of abnormal mitochondria (Fig. 6B). We then analyzed a publicly available microarray data set (GSE30723, https://www.ncbi.nlm.nih.gov/geo/query/acc.cgi?acc=GSE30723) of human AMs that were infected with influenza PR8 strain for 4 or 24 hours (46). TFAM expression in infected AMs was decreased compared to uninfected AM (Fig. 6C). In consistency, GSEA revealed that there was a decreased enrichment of mitochondrial OXPHOS-related genes in influenza-infected AMs (24 hour) compared to those of uninfected AM (Fig. 6D). Together, these data suggested that influenza infection may impair TFAM expression, thereby causing defective mitochondrial fitness and function in AMs.

Discussion

Tissue-resident macrophages are important in regulating tissue homeostasis and inflammation, and are essential for tissue-specific function and the host protection from infection. Better understanding on the molecular and metabolic pathways regulating tissue-resident macrophage development, maintenance and function will aid to identify macrophage-targeting therapies for various acute and chronic diseases (41, 47, 48). Here we have identified a critical role of TFAM in regulating AM proliferation and phenotypes, thereby providing the first genetic evidence on the roles of mitochondrial metabolism in regulating AM maintenance *in vivo*.

A number of factors have been identified to be important in AM development, maintenance and/or function, including GM-CSF, TGF-β, Bach2, PPARγ and mTORC1 etc. Particularly, PPARγ is considered a “master” regulator of AM development and function, although the underlying mechanisms by which PPARγ regulates AM development and function remain to be fully elucidated. Interestingly, PPARγ deficient AMs had altered mitochondrial and lipid metabolism (1, 14), suggesting that mitochondrial metabolism may be important for AM development and/or maintenance. Furthermore, Bach2-deficient AMs had altered lipid metabolism, leading to enhanced lipid accumulation inside the cells (15). Consistent with these findings, we recently have shown that the inhibition of mitochondrial electron transport chain (ETC), but not the inhibition of glycolysis, impaired AM proliferation and

self-renewal *in vivo* (49). Using genetic deficiency of TFAM, here we have provided strong evidence that mitochondrial fitness and metabolism are critical for AM maintenance and function. Interestingly, CD11c-cre mediated TFAM deficiency did not diminish pulmonary DC numbers. Furthermore, Ubc-creERT2 mediated acute depletion of TFAM impaired AM maintenance but not DCs, interstitial macrophages and other immune cell types, arguing that TFAM is selectively required for AM homeostasis in the respiratory tract. The exact reason underlying this phenomenon requires further investigation. However, AMs are the only immune cell type that directly expose to the ambient air in adult mouse lung during homeostasis. Furthermore, alveolar space is full of lipids and lipid-rich surfactant, which are phagocytized by AMs (but is almost deficient with glucose) (36, 37). Therefore, AMs may be selectively adapted to use mitochondrial metabolism and fatty acid oxidation as their energy source due to the oxygen-rich and lipid-rich environment in the alveolar space. Consistent with this idea, TFAM deficiency leads to increased accumulation of lipid inside the cells, most likely due to the impaired lipid oxidation by mitochondria. Of note, TFAM deficiency did not impair AM precursor development and their differentiation into AMs, suggesting that AMs may gradually adapt to the airway environment during lung development and maturation process, which normally end at 4 weeks after birth (50, 51).

AMs are primarily maintained through proliferation and self-renewal independent of monocyte infiltration in the adulthood during homeostasis. Although still controversial, a recent report suggests that monocytes may contribute to a significant portion of AMs in adult mice, and their contributions to AM compartment gradually increase during aging (52). To this end, a recent report has found that TFAM deficiency did not decrease AM numbers in aged mice (53). We did not explore the roles of TFAM in regulating AM compartment in our mouse colony due to the time limitation. Nevertheless, it is possible that monocytes eventually infiltrate into the empty AM niche, differentiate into monocyte-derived AMs and compensate the loss of embryonic-derived AMs in CD11c Cre *Tfam*$^{fl/fl}$ mice. Additionally, it is possible that AMs may eventually adapt to impaired mitochondrial metabolism and use other metabolic pathways for their energy source and homeostatic proliferation. These possibilities require further studies.

Macrophage metabolism is critical in regulating pro- and anti-inflammatory responses of macrophages (54–57). For example, glycolysis is critical for macrophage inflammatory cytokine production, while mitochondrial metabolism and fatty acid oxidation promotes M2 macrophage differentiation and the production of anti-inflammatory cytokines such as IL-10 (58, 59). As the resident macrophages in lung alveoli, AMs exhibit M2 macrophage features and are considered as immunosuppressive during homeostasis. We believe that TFAM-mediated mitochondrial metabolism is vital to maintain the immuno-quiescent state of AMs as TFAM-deficiency resulted in increased expression of inflammatory gene sets. On the other hand, AMs can rapidly upregulate inflammatory responses following viral exposure (60). To this end, we have shown before that AMs from influenza-infected mice exhibited decreased mitochondrial fitness (29), although whether influenza can directly impair AM fitness is not known. To this end, influenza virus is known to cause impaired mitochondrial fitness, diminished lipid oxidation and mitochondrial DNA release in epithelial and/or structural cells (61, 62). We have confirmed in AMs that direct influenza infection caused mitochondrial abnormality, which is associated with decreased TFAM expression. Since

TFAM deficiency could result in increased inflammatory responses, it is possible that the impaired TFAM expression in influenza-exposed AMs may help to prime inflammatory responses in AMs following infection *in vivo*. Furthermore, AM inflammation could ignite and contribute exuberant pulmonary inflammation following severe influenza infection (63, 64). It is thus possible that agents that can increase mitochondrial fitness may be used therapeutically to dampen exaggerated pulmonary inflammatory responses mediated by the exuberant macrophage responses in the future.

In summary, our data have shown the first genetic evidence on the roles of mitochondrial metabolism in regulating resident macrophage self-renewal in the respiratory tract. Furthermore, our data have provided insights on the potential beneficial roles of the restoration of mitochondrial function for therapeutic interventions of respiratory viral infection.

Limitation of the study

CD11c is also expressed by respiratory DCs. We found that TFAM deficiency did not impair DCs numbers or subsequent antigen-specific T cell responses following influenza infection, indicating that TFAM deficiency in $CD11c^+$ cells may not impair DC quantity and functions following influenza infection. However, we can not definitively rule out the possibility that TFAM-deficiency in DCs or other uncharacterized lung $CD11c^+$ cells, other than AMs, may contribute to the observed phenotypes (excessive pulmonary inflammation and increased mortality) in the $CD11c^{cre}Tfam^{fl/fl}$ mice following influenza infection. Further studies are required to address this limitation.

Supplementary Material

Refer to Web version on PubMed Central for supplementary material.

ACKNOWLEDGEMENTS

We thank Mayo flow cytometry core for assistance.

This study was funded by the NIH grants AI112844, AI147394, AG069264 and AG047156 and Mayo Clinic Kogod Aging Center and Center for Biomedical Discovery Funds to J.S.

References

1. Guilliams M, De Kleer I, Henri S, Post S, Vanhoutte L, De Prijck S, Deswarte K, Malissen B, Hammad H, and Lambrecht BN. 2013. Alveolar macrophages develop from fetal monocytes that differentiate into long-lived cells in the first week of life via GM-CSF. J Exp Med 210: 1977–1992. [PubMed: 24043763]
2. Hoeffel G, Chen J, Lavin Y, Low D, Almeida FF, See P, Beaudin AE, Lum J, Low I, Forsberg EC, Poidinger M, Zolezzi F, Larbi A, Ng LG, Chan JK, Greter M, Becher B, Samokhvalov IM, Merad M, and Ginhoux F. 2015. C-Myb(+) erythro-myeloid progenitor-derived fetal monocytes give rise to adult tissue-resident macrophages. Immunity 42: 665–678. [PubMed: 25902481]
3. Kopf M, Schneider C, and Nobs SP. 2015. The development and function of lung-resident macrophages and dendritic cells. Nat Immunol 16: 36–44. [PubMed: 25521683]
4. Mass E, Ballesteros I, Farlik M, Halbritter F, Gunther P, Crozet L, Jacome-Galarza CE, Handler K, Klughammer J, Kobayashi Y, Gomez-Perdiguero E, Schultze JL, Beyer M, Bock C, and Geissmann

F. 2016. Specification of tissue-resident macrophages during organogenesis. Science 353: aaf4238. [PubMed: 27492475]

5. Hussell T, and Bell TJ. 2014. Alveolar macrophages: plasticity in a tissue-specific context. Nat Rev Immunol 14: 81–93. [PubMed: 24445666]
6. Suzuki T, Sakagami T, Rubin BK, Nogee LM, Wood RE, Zimmerman SL, Smolarek T, Dishop MK, Wert SE, Whitsett JA, Grabowski G, Carey BC, Stevens C, van der Loo JC, and Trapnell BC. 2008. Familial pulmonary alveolar proteinosis caused by mutations in CSF2RA. J Exp Med 205: 2703–2710. [PubMed: 18955570]
7. Trapnell BC, Nakata K, Bonella F, Campo I, Griese M, Hamilton J, Wang T, Morgan C, Cottin V, and McCarthy C. 2019. Pulmonary alveolar proteinosis. Nat Rev Dis Primers 5: 16. [PubMed: 30846703]
8. Kim HM, Lee YW, Lee KJ, Kim HS, Cho SW, van Rooijen N, Guan Y, and Seo SH. 2008. Alveolar macrophages are indispensable for controlling influenza viruses in lungs of pigs. J Virol 82: 4265–4274. [PubMed: 18287245]
9. Purnama CN, L S; Tetlak P; Aphrilia S; Kandasamy M; Baalasubramanian S; Karialainen K; Ruedl C 2003. Transient ablation of alveolar macrophages leads massive pathology of influenza infection without affecting cellular adaptive immunity. Eur J Immunol 44: 2003–2012.
10. Cardani A, Boulton A, Kim TS, and Braciale TJ. 2017. Alveolar Macrophages Prevent Lethal Influenza Pneumonia By Inhibiting Infection Of Type-1 Alveolar Epithelial Cells. PLoS Pathog 13: e1006140. [PubMed: 28085958]
11. Schneider C, Nobs SP, Heer AK, Kurrer M, Klinke G, van Rooijen N, Vogel J, and Kopf M. 2014. Alveolar macrophages are essential for protection from respiratory failure and associated morbidity following influenza virus infection. PLoS Pathog 10: e1004053. [PubMed: 24699679]
12. Laidlaw BJ, Decman V, Ali MA, Abt MC, Wolf AI, Monticelli LA, Mozdzanowska K, Angelosanto JM, Artis D, Erikson J, and Wherry EJ. 2013. Cooperativity between CD8+ T cells, non-neutralizing antibodies, and alveolar macrophages is important for heterosubtypic influenza virus immunity. PLoS Pathog 9: e1003207. [PubMed: 23516357]
13. Huang S, Zhu B, Cheon IS, Goplen NP, Jiang L, Zhang R, Peebles RS, Mack M, Kaplan MH, Limper AH, and Sun J. 2019. PPAR-gamma in Macrophages Limits Pulmonary Inflammation and Promotes Host Recovery following Respiratory Viral Infection. J Virol 93: e00030–19. [PubMed: 30787149]
14. Yu X, Buttgereit A, Lelios I, Utz SG, Cansever D, Becher B, and Greter M. 2017. The Cytokine TGF-beta Promotes the Development and Homeostasis of Alveolar Macrophages. Immunity 47: 903–912 e904. [PubMed: 29126797]
15. Nakamura A, Ebina-Shibuya R, Itoh-Nakadai A, Muto A, Shima H, Saigusa D, Aoki J, Ebina M, Nukiwa T, and Igarashi K. 2013. Transcription repressor Bach2 is required for pulmonary surfactant homeostasis and alveolar macrophage function. J Exp Med 210: 2191–2204. [PubMed: 24127487]
16. Rauschmeier R, Gustafsson C, Reinhardt A, N AG, Tortola L, Cansever D, Subramanian S, Taneja R, Rossner MJ, Sieweke MH, Greter M, Mansson R, Busslinger M, and Kreslavsky T. 2019. Bhlhe40 and Bhlhe41 transcription factors regulate alveolar macrophage self-renewal and identity. EMBO J 38: e101233. [PubMed: 31414712]
17. Suwankitwat N, Libby S, Liggitt HD, Avalos A, Ruddell A, Rosch JW, Park H, and Iritani BM. 2021. The actin-regulatory protein Hem-1 is essential for alveolar macrophage development. J Exp Med 218: e20200472. [PubMed: 33600594]
18. Kawasaki T, Ito K, Miyata H, Akira S, and Kawai T. 2017. Deletion of PIKfyve alters alveolar macrophage populations and exacerbates allergic inflammation in mice. EMBO J 36: 1707–1718. [PubMed: 28533230]
19. Wang Q, Chen S, Li T, Yang Q, Liu J, Tao Y, Meng Y, Chen J, Feng X, Han Z, Shi M, Huang H, Han M, and Jiang E. 2021. Critical Role of Lkb1 in the Maintenance of Alveolar Macrophage Self-Renewal and Immune Homeostasis. Front Immunol 12: 629281. [PubMed: 33968022]
20. Deng W, Yang J, Lin X, Shin J, Gao J, and Zhong XP. 2017. Essential Role of mTORC1 in Self-Renewal of Murine Alveolar Macrophages. J Immunol 198: 492–504. [PubMed: 27881705]

21. Weinberg SE, Sena LA, and Chandel NS. 2015. Mitochondria in the regulation of innate and adaptive immunity. Immunity 42: 406–417. [PubMed: 25786173]
22. West AP, Shadel GS, and Ghosh S. 2011. Mitochondria in innate immune responses. Nat Rev Immunol 11: 389–402. [PubMed: 21597473]
23. Li C, Zhu B, Son YM, Wang Z, Jiang L, Xiang M, Ye Z, Beckermann KE, Wu Y, Jenkins JW, Siska PJ, Vincent BG, Prakash YS, Peikert T, Edelson BT, Taneja R, Kaplan MH, Rathmell JC, Dong H, Hitosugi T, and Sun J. 2019. The Transcription Factor Bhlhe40 Programs Mitochondrial Regulation of Resident CD8(+) T Cell Fitness and Functionality. Immunity 51: 491–507 e497. [PubMed: 31533057]
24. Matilainen O, Quiros PM, and Auwerx J. 2017. Mitochondria and Epigenetics - Crosstalk in Homeostasis and Stress. Trends Cell Biol 27: 453–463. [PubMed: 28274652]
25. Campbell CT, Kolesar JE, and Kaufman BA. 2012. Mitochondrial transcription factor A regulates mitochondrial transcription initiation, DNA packaging, and genome copy number. Biochim Biophys Acta 1819: 921–929. [PubMed: 22465614]
26. Larsson NG, Wang J, Wilhelmsson H, Oldfors A, Rustin P, Lewandoski M, Barsh GS, and Clayton D. 1998. Mitochondrial transcription factor A is necessary for mtDNA maintenance and embryogenesis in mice. Nat Genet 18: 231–236. [PubMed: 9500544]
27. Song Y, Hussain T, Wang J, Liao Y, Yue R, Sabir N, Zhao D, and Zhou X. 2020. Mitochondrial Transcription Factor A Regulates Mycobacterium bovis-Induced IFN-beta Production by Modulating Mitochondrial DNA Replication in Macrophages. J Infect Dis 221: 438–448. [PubMed: 31495880]
28. West AP, Khoury-Hanold W, Staron M, Tal MC, Pineda CM, Lang SM, Bestwick M, Duguay BA, Raimundo N, MacDuff DA, Kaech SM, Smiley JR, Means RE, Iwasaki A, and Shadel GS. 2015. Mitochondrial DNA stress primes the antiviral innate immune response. Nature 520: 553–557. [PubMed: 25642965]
29. Zhu B, Wu Y, Huang S, Zhang R, Son YM, Li C, Cheon IS, Gao X, Wang M, Chen Y, Zhou X, Nguyen Q, Phan AT, Behl S, Taketo MM, Mack M, Shapiro VS, Zeng H, Ebihara H, Mullon JJ, Edell ES, Reisenauer JS, Demirel N, Kern RM, Chakraborty R, Cui W, Kaplan MH, Zhou X, Goldrath AW, and Sun J. 2021. Uncoupling of macrophage inflammation from self-renewal modulates host recovery from respiratory viral infection. Immunity 54: 1200–1218 e1209. [PubMed: 33951416]
30. Zhu B, Zhang R, Li C, Jiang L, Xiang M, Ye Z, Kita H, Melnick AM, Dent AL, and Sun J. 2019. BCL6 modulates tissue neutrophil survival and exacerbates pulmonary inflammation following influenza virus infection. Proc Natl Acad Sci U S A 116: 11888–11893. [PubMed: 31138703]
31. Ruzankina Y, Pinzon-Guzman C, Asare A, Ong T, Pontano L, Cotsarelis G, Zediak VP, Velez M, Bhandoola A, and Brown EJ. 2007. Deletion of the developmentally essential gene ATR in adult mice leads to age-related phenotypes and stem cell loss. Cell Stem Cell 1: 113–126. [PubMed: 18371340]
32. Sun J, Madan R, Karp CL, and Braciale TJ. 2009. Effector T cells control lung inflammation during acute influenza virus infection by producing IL-10. Nat Med 15: 277–284. [PubMed: 19234462]
33. Sohn YS, Tamir S, Song L, Michaeli D, Matouk I, Conlan AR, Harir Y, Holt SH, Shulaev V, Paddock ML, Hochberg A, Cabanchick IZ, Onuchic JN, Jennings PA, Nechushtai R, and Mittler R. 2013. NAF-1 and mitoNEET are central to human breast cancer proliferation by maintaining mitochondrial homeostasis and promoting tumor growth. Proc Natl Acad Sci U S A 110: 14676–14681. [PubMed: 23959881]
34. Stranges PB, Watson J, Cooper CJ, Choisy-Rossi CM, Stonebraker AC, Beighton RA, Hartig H, Sundberg JP, Servick S, Kaufmann G, Fink PJ, and Chervonsky AV. 2007. Elimination of antigen-presenting cells and autoreactive T cells by Fas contributes to prevention of autoimmunity. Immunity 26: 629–641. [PubMed: 17509906]
35. Chakarov S, Lim HY, Tan L, Lim SY, See P, Lum J, Zhang X, Foo S, Nakamizo S, Duan K, Kong WT, Gentek R, Balachander A, Carbajo D, Bleriot C, Malleret B, Tam JKC, Baig S, Shabeer M, and Ginhoux F. 2019. Two distinct interstitial macrophage populations coexist across tissues in specific subtissular niches. Science 363: 1190–1203.

36. Izquierdo HM, Brandi P, Gomez MJ, Conde-Garrosa R, Priego E, Enamorado M, Martinez-Cano S, Sanchez I, Conejero L, Jimenez-Carretero D, Martin-Puig S, Guilliams M, and Sancho D. 2018. Von Hippel-Lindau Protein Is Required for Optimal Alveolar Macrophage Terminal Differentiation, Self-Renewal, and Function. Cell Rep 24: 1738–1746. [PubMed: 30110631]
37. Schneider C, Nobs SP, Kurrer M, Rehrauer H, Thiele C, and Kopf M. 2014. Induction of the nuclear receptor PPAR-gamma by the cytokine GM-CSF is critical for the differentiation of fetal monocytes into alveolar macrophages. Nat Immunol 15: 1026–1037. [PubMed: 25263125]
38. Tontonoz P, and Spiegelman BM. 2008. Fat and beyond: the diverse biology of PPARgamma. Annu Rev Biochem 77: 289–312. [PubMed: 18518822]
39. van de Laar L, Saelens W, De Prijck S, Martens L, Scott CL, Van Isterdael G, Hoffmann E, Beyaert R, Saeys Y, Lambrecht BN, and Guilliams M. 2016. Yolk Sac Macrophages, Fetal Liver, and Adult Monocytes Can Colonize an Empty Niche and Develop into Functional Tissue-Resident Macrophages. Immunity 44: 755–768. [PubMed: 26992565]
40. Hochreiter-Hufford A, and Ravichandran KS. 2013. Clearing the dead: apoptotic cell sensing, recognition, engulfment, and digestion. Cold Spring Harb Perspect Biol 5: a008748. [PubMed: 23284042]
41. Epelman S, Lavine KJ, and Randolph GJ. 2014. Origin and functions of tissue macrophages. Immunity 41: 21–35. [PubMed: 25035951]
42. Newton AH, Cardani A, and Braciale TJ. 2016. The host immune response in respiratory virus infection: balancing virus clearance and immunopathology. Semin Immunopathol 38: 471–482. [PubMed: 26965109]
43. Kumagai Y, Takeuchi O, Kato H, Kumar H, Matsui K, Morii E, Aozasa K, Kawai T, and Akira S. 2007. Alveolar macrophages are the primary interferon-alpha producer in pulmonary infection with RNA viruses. Immunity 27: 240–252. [PubMed: 17723216]
44. Wang ZW, S.; Goplen N; Li C; Cheon I; Dai Q; Huang S; Shan J; Ma C; Ye Z; Xiang M; Limper A; Porquera E; KOhlmeler J; Kaplan M; Zhang N; Johnson A; Vassallo R; Sun J 2019. PD-1hi CD8+ resident memory T cells balance immunity and fibrotic sequelae. Sci Immunol 4:eaaw1217. [PubMed: 31201259]
45. Gwyer Findlay E, and Hussell T. 2012. Macrophage-mediated inflammation and disease: a focus on the lung. Mediators Inflamm 2012: 140937. [PubMed: 23304058]
46. Wang J, Nikrad MP, Phang T, Gao B, Alford T, Ito Y, Edeen K, Travanty EA, Kosmider B, Hartshorn K, and Mason RJ. 2011. Innate immune response to influenza A virus in differentiated human alveolar type II cells. Am J Respir Cell Mol Biol 45: 582–591. [PubMed: 21239608]
47. Suzuki T, Arumugam P, Sakagami T, Lachmann N, Chalk C, Sallese A, Abe S, Trapnell C, Carey B, Moritz T, Malik P, Lutzko C, Wood RE, and Trapnell BC. 2014. Pulmonary macrophage transplantation therapy. Nature 514: 450–454. [PubMed: 25274301]
48. Ginhoux F, and Guilliams M. 2016. Tissue-Resident Macrophage Ontogeny and Homeostasis. Immunity 44: 439–449. [PubMed: 26982352]
49. Woods PS, Kimmig LM, Meliton AY, Sun KA, Tian Y, O'Leary EM, Gokalp GA, Hamanaka RB, and Mutlu GM. 2020. Tissue-Resident Alveolar Macrophages Do Not Rely on Glycolysis for LPS-induced Inflammation. Am J Respir Cell Mol Biol 62: 243–255. [PubMed: 31469581]
50. Joshi N, Walter JM, and Misharin AV. 2018. Alveolar Macrophages. Cell Immunol 330: 86–90. [PubMed: 29370889]
51. Jenkins SJ, and Allen JE. 2021. The expanding world of tissue-resident macrophages. Eur J Immunol 51:1882–1896. [PubMed: 34107057]
52. McQuattie-Pimentel AC, Ren Z, Joshi N, Watanabe S, Stoeger T, Chi M, Lu Z, Sichizya L, Aillon RP, Chen CI, Soberanes S, Chen Z, Reyfman PA, Walter JM, Anekalla KR, Davis JM, Helmin KA, Runyan CE, Abdala-Valencia H, Nam K, Meliton AY, Winter DR, Morimoto RI, Mutlu GM, Bharat A, Perlman H, Gottardi CJ, Ridge KM, Chandel NS, Sznajder JI, Balch WE, Singer BD, Misharin AV, and Budinger GRS. 2021. The lung microenvironment shapes a dysfunctional response of alveolar macrophages in aging. J Clin Invest 131: e140299. [PubMed: 33586677]
53. Ma J, Sabir N, Wack A, Lu Z, Kihshen H, Sichizya L, Misharin AV, and Budinger GRS. 2020. Mitochondrial Transcription Factor A (TFAM) Is Not Necessary for Alveolar Macrophage Survival and Function During Aging. Am J Respir Crit Care Med 201: A4391–A4391.

54. Van den Bossche J, O'Neill LA, and Menon D. 2017. Macrophage Immunometabolism: Where Are We (Going)? Trends Immunol 38: 395–406. [PubMed: 28396078]
55. Biswas SK, and Mantovani A. 2012. Orchestration of metabolism by macrophages. Cell Metab 15: 432–437. [PubMed: 22482726]
56. Watanabe S, Alexander M, Misharin AV, and Budinger GRS. 2019. The role of macrophages in the resolution of inflammation. J Clin Invest 129: 2619–2628. [PubMed: 31107246]
57. O'Neill LA, and Pearce EJ. 2016. Immunometabolism governs dendritic cell and macrophage function. J Exp Med 213: 15–23. [PubMed: 26694970]
58. Semba H, Takeda N, Isagawa T, Sugiura Y, Honda K, Wake M, Miyazawa H, Yamaguchi Y, Miura M, Jenkins DM, Choi H, Kim JW, Asagiri M, Cowburn AS, Abe H, Soma K, Koyama K, Katoh M, Sayama K, Goda N, Johnson RS, Manabe I, Nagai R, and Komuro I. 2016. HIF-1alpha-PDK1 axis-induced active glycolysis plays an essential role in macrophage migratory capacity. Nat Commun 7: 11635. [PubMed: 27189088]
59. Ghoneim HE, Thomas PG, and McCullers JA. 2013. Depletion of alveolar macrophages during influenza infection facilitates bacterial superinfections. J Immunol 191: 1250–1259. [PubMed: 23804714]
60. Aegerter H, Kulikauskaite J, Crotta S, Patel H, Kelly G, Hessel EM, Mack M, Beinke S, and Wack A. 2020. Influenza-induced monocyte-derived alveolar macrophages confer prolonged antibacterial protection. Nat Immunol 21: 145–157. [PubMed: 31932810]
61. Keshavarz M, Solaymani-Mohammadi F, Namdari H, Arjeini Y, Mousavi MJ, and Rezaei F. 2020. Metabolic host response and therapeutic approaches to influenza infection. Cell Mol Biol Lett 25: 15. [PubMed: 32161622]
62. Moriyama M, Koshiba T, and Ichinohe T. 2019. Influenza A virus M2 protein triggers mitochondrial DNA-mediated antiviral immune responses. Nat Commun 10: 4624. [PubMed: 31604929]
63. Tate MD, Pickett DL, van Rooijen N, Brooks AG, and Reading PC. 2010. Critical role of airway macrophages in modulating disease severity during influenza virus infection of mice. J Virol 84: 7569–7580. [PubMed: 20504924]
64. Archambaud C, Salcedo SP, Lelouard H, Devilard E, de Bovis B, Van Rooijen N, Gorvel JP, and Malissen B. 2010. Contrasting roles of macrophages and dendritic cells in controlling initial pulmonary Brucella infection. Eur J Immunol 40: 3458–3471. [PubMed: 21108467]

Key points:

- TFAM deficiency impairs alveolar macrophage (AM) mitochondria metabolism
- TFAM is required for AM self-renewal and maintenance
- Viral infection leads to decreased AM TFAM expression and mitochondrial fitness

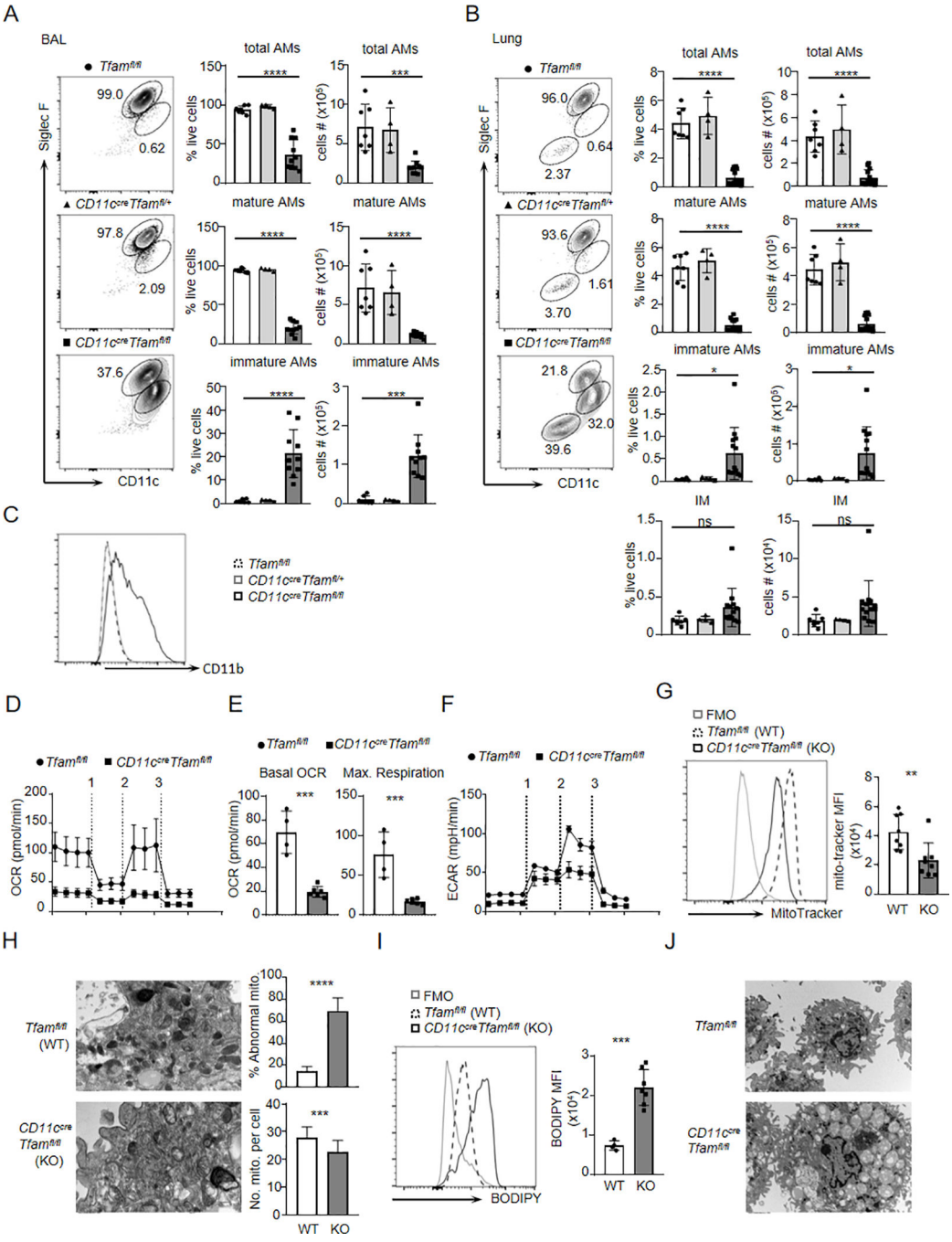

FIGURE 1. TFAM is required for the maintenance of mature AMs in adult mice.

(**A** and **B**) Flow cytometry analysis of AMs from *Tfam*$^{fl/fl}$, *CD11c*^{cre}*Tfam*$^{fl/+}$ and *CD11c*^{cre}*Tfam*$^{fl/fl}$ adult mice. Representative flow cytometry plots and graphs show the percentage and cell numbers of total AMs, mature AMs, immature AMs and IM (interstitial macrophages) in BAL (A) and lung (B). (**C**) Histogram plot for CD11b expression of AMs in the BAL from *Tfam*$^{fl/fl}$, *CD11c*^{cre}*Tfam*$^{fl/+}$ and *CD11c*^{cre}*Tfam*$^{fl/fl}$ mice. (**D**) Real-time OCRs of AMs in BAL from *Tfam*$^{fl/fl}$ and *CD11c*^{cre}*Tfam*$^{fl/fl}$ mice followed by sequential treatment with Oligomycin (1), FCCP (2) and Antimycin A/Rotenone (3). (**E**) Quantitative

changes for the basal OCR and max. respiratory. (**F**) Real-time ECAR of AMs in BAL from *Tfam*$^{fl/fl}$ and *CD11c*^{cre}*Tfam*$^{fl/fl}$ mice followed by sequential treatment with Glucose (1), Oligomycin (2) and 2-DG (3). (**G**) Representative flow cytometry plots and graphs show MFI (mean fluorescence intensity) of mitoTracker Green of AMs in the BAL from *Tfam*$^{fl/fl}$ and *CD11c*^{cre}*Tfam*$^{fl/fl}$ mice. (**H**) Transmission electron microscopy images of AMs in BAL from *Tfam*$^{fl/fl}$ and *CD11c*^{cre}*Tfam*$^{fl/fl}$ mice. Scale bars, 1 μm. Quantification of mitochondrial numbers and percentages of abnormal mitochondria in AMs is shown on the right. (**I**) Flow cytometry plots and graphs for MFI of BODIPY from AMs in the BAL. (**J**) Transmission electron microscopy images of lipid droplet in AMs from *Tfam*$^{fl/fl}$ and *CD11c*^{cre}*Tfam*$^{fl/fl}$ mice. Scale bars, 5 μm. Data are presented as arithmetic means ± SD. *, $p < 0.05$; **, $p < 0.01$; ***, $p < 0.001$.

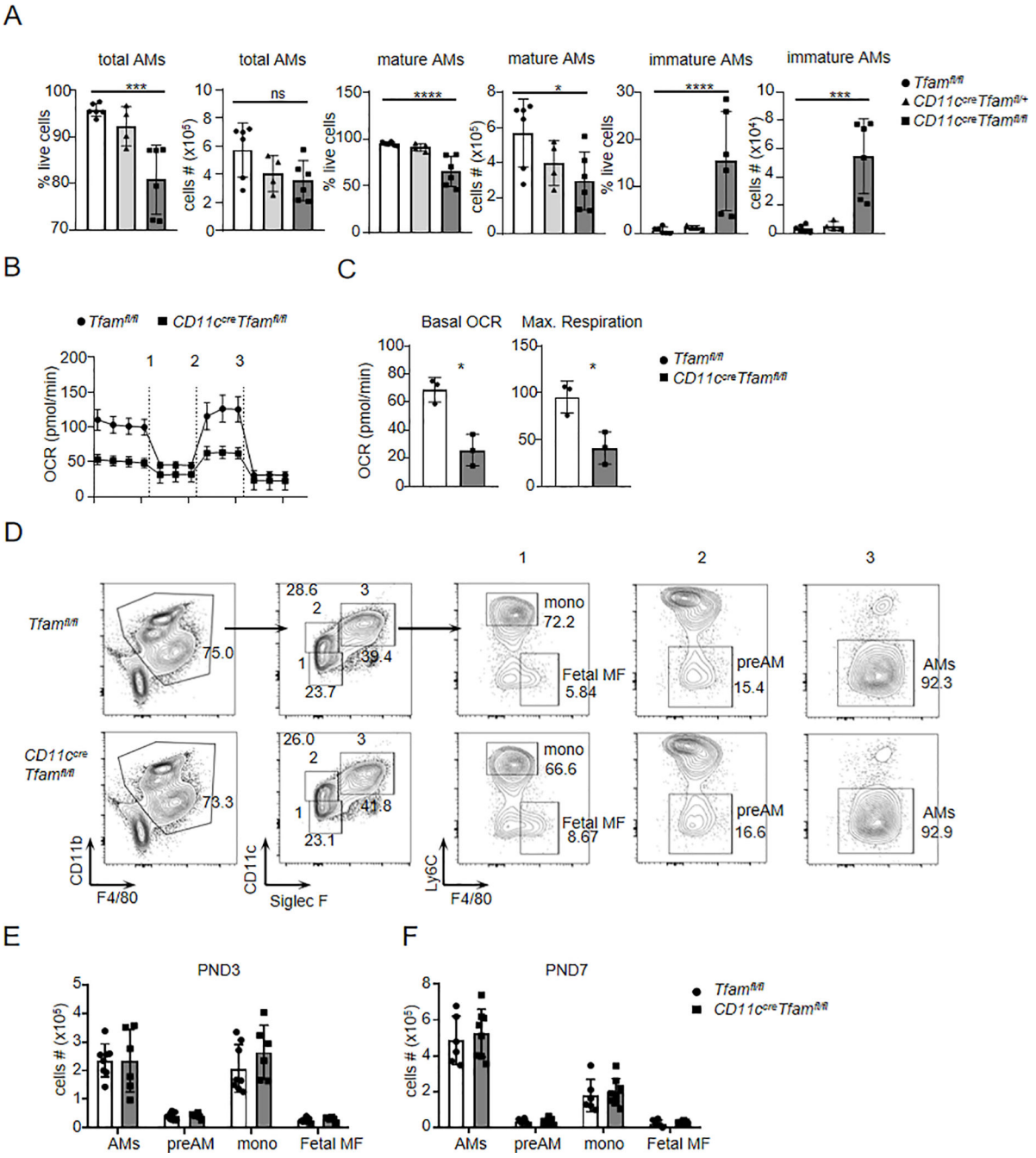

FIGURE 2. TFAM does not affect the development of AMs.

(**A**) The percentage and total cell numbers of total AMs, mature AMs and immature AMs in BAL from *Tfam*$^{fl/fl}$, *CD11c*^{cre}*Tfam*$^{fl/+}$ and *CD11c*^{cre}*Tfam*$^{fl/fl}$ mice at the age of 3–4 weeks. (**B** and **C**) Real-time OCRs of AMs in BAL from *Tfam*$^{fl/fl}$ and *CD11c*^{cre}*Tfam*$^{fl/fl}$ mice at the age of 3–4 weeks followed by sequential treatment with Oligomycin, FCCP and Antimycin A/Rotenone (B). The basal OCR and max. respiratory were shown (C). (**D**) Representative flow cytometry gating scheme of fetal macrophages (MF), fetal monocytes (mono), pre-AM and mature AMs in whole lung tissue from *Tfam*$^{fl/fl}$ and *CD11c*^{cre}*Tfam*$^{fl/fl}$

pups at PND3. Prior gated on $CD45^+$ live cells. (**E** and **F**) The cell numbers of fetal macrophages, fetal monocytes, pre-AM and mature AMs in whole lung tissue from *Tfam*$^{fl/fl}$ and *CD11c*^{cre}*Tfam*$^{fl/fl}$ pups at PND3 (E) and PND7 (F). Data are presented as arithmetic means ± SD. *, $p < 0.05$; **, $p < 0.01$; ***, $p < 0.001$.

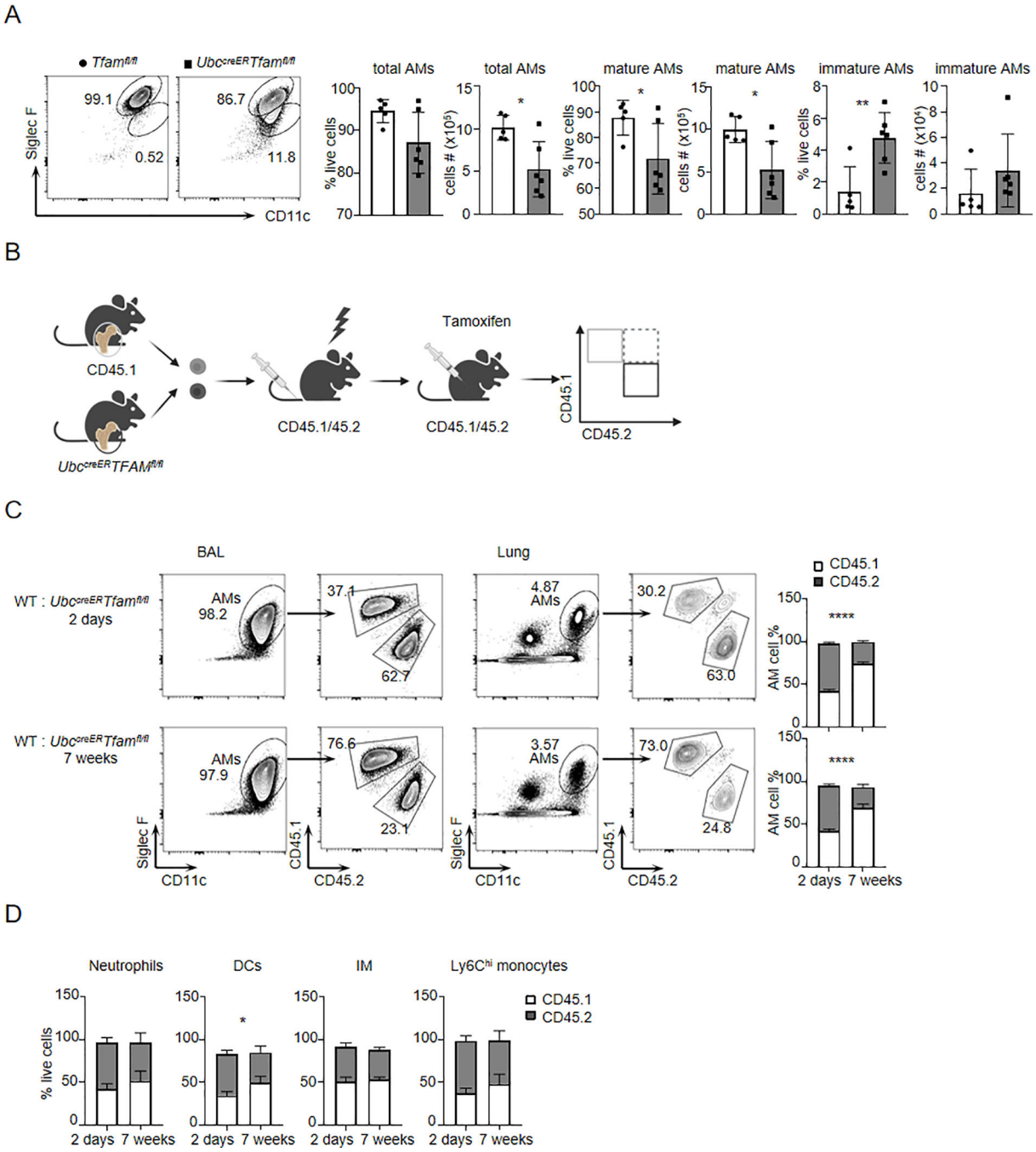

FIGURE 3. TFAM is required for AM maintenance.

(**A**) Representative flow cytometry plots and graphs of total AMs, mature AMs and immature AMs from *Tfam*$^{fl/fl}$ and *Ubc*^{creER}*Tfam*$^{fl/fl}$ mice at the 3–4 weeks post tamoxifen treatment. (**B**) The schematic of experimental design for the bone marrow chimeric mice. (**C**) Representative flow cytometry plots and frequencies of CD45.1^{+} and CD45.2^{+} AMs in BAL and lung fraction of chimeras at 2 days and 7 weeks post last tamoxifen treatment. (**D**) The frequencies CD45.1^{+} and CD45.2^{+} neutrophils, DCs, IM, and Ly6C^{hi} monocytes in lung

tissue of chimeras at 2 days and 7 weeks post tamoxifen treatment. Data are presented as arithmetic means ± SD. *, $p < 0.05$; **, $p < 0.01$; ***, $p < 0.001$.

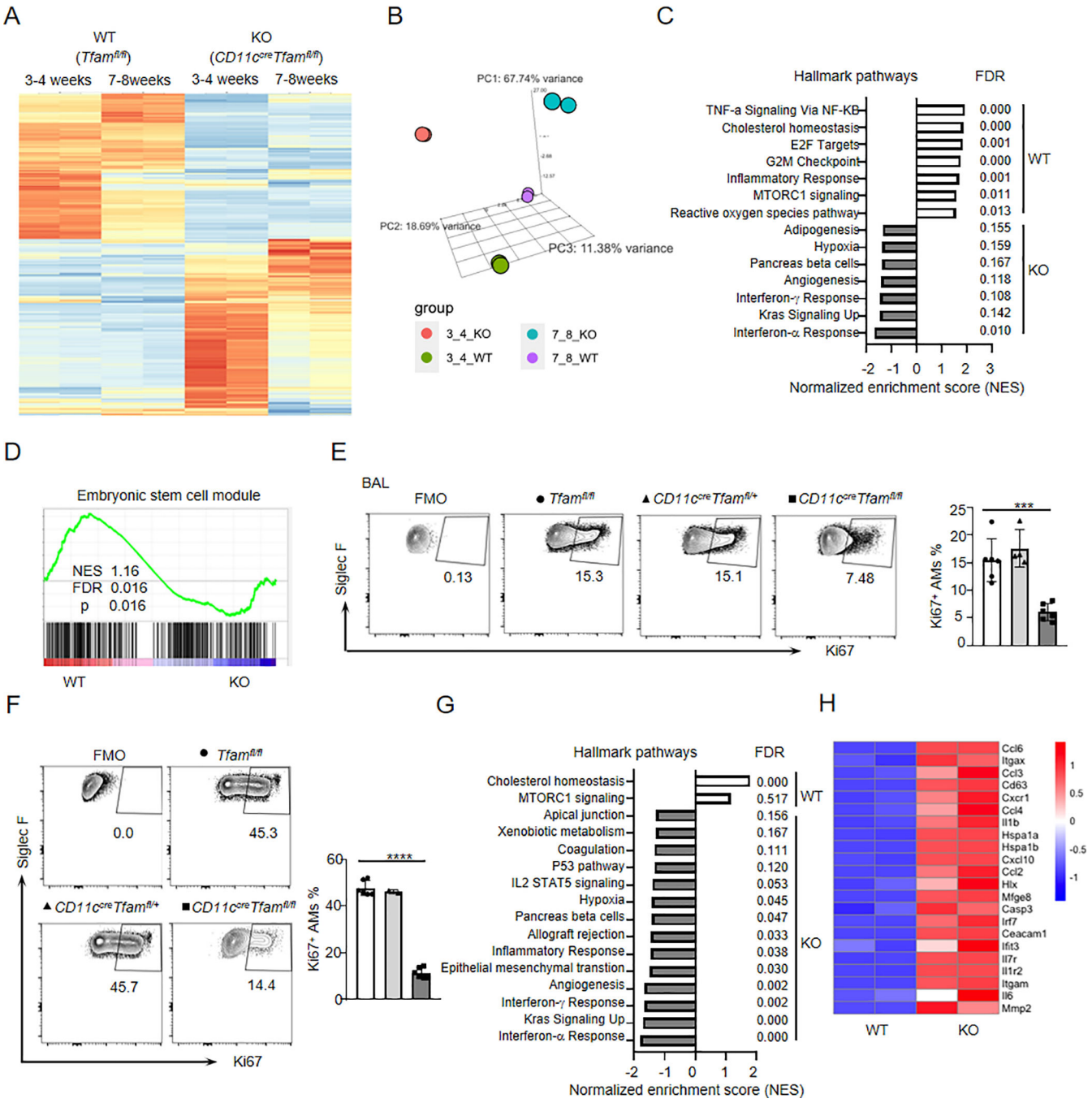

FIGURE 4. TFAM controls AM self-renewal and function.

(**A**) Heat map showing top 500 differentially expressed genes in AMs from *Tfam*$^{fl/fl}$ (42) and *CD11c*^{cre}*Tfam*$^{fl/fl}$ (KO) mice at the age of 3–4 and 7–8 weeks. Yellow color indicates a higher expression while blue refers to a lower expression. (**B**) Principle component analysis (PCA) was performed on transcriptome of AMs from *Tfam*$^{fl/fl}$ and *CD11c*^{cre}*Tfam*$^{fl/fl}$ mice at the age of 3–4 and 7–8 weeks. (**C**) Normalized enrichment scores of GSEA from the hallmark gene sets in the molecular signatures database, showing the most significantly enriched gene sets in AMs from *Tfam*$^{fl/fl}$ and *CD11c*^{cre}*Tfam*$^{fl/fl}$

mice at the age of 3–4 weeks. (**D**) Enrichment plot of embryonic stem cell module from GSEA of AMs from *Tfam*$^{fl/fl}$ and *CD11c*^{cre}*Tfam*$^{fl/fl}$ mice at the age of 3–4 weeks. (**E** and **F**) Flow cytometry plots and frequencies of Ki67^{+} AMs in BAL (E) *in vivo* and *in vitro* (F) from *Tfam*$^{fl/fl}$, *CD11c*^{cre}*Tfam*$^{fl/+}$ and *CD11c*^{cre}*Tfam*$^{fl/fl}$ mice at the age of 3–4 weeks. (**G**) Normalized enrichment scores of GSEA from the hallmark gene sets in the molecular signatures database, showing the most significantly enriched gene sets in AMs from *Tfam*$^{fl/fl}$ and *CD11c*^{cre}*Tfam*$^{fl/fl}$ mice at the age of 7–8 weeks. (**H**) Heat map showing differentially expressed genes associated with inflammatory responses in AMs from *Tfam*$^{fl/fl}$ and *CD11c*^{cre}*Tfam*$^{fl/fl}$ mice at the age of 7–8 weeks. Data are presented as arithmetic means ± SD. *, $p < 0.05$; **, $p < 0.01$; ***, $p < 0.001$.

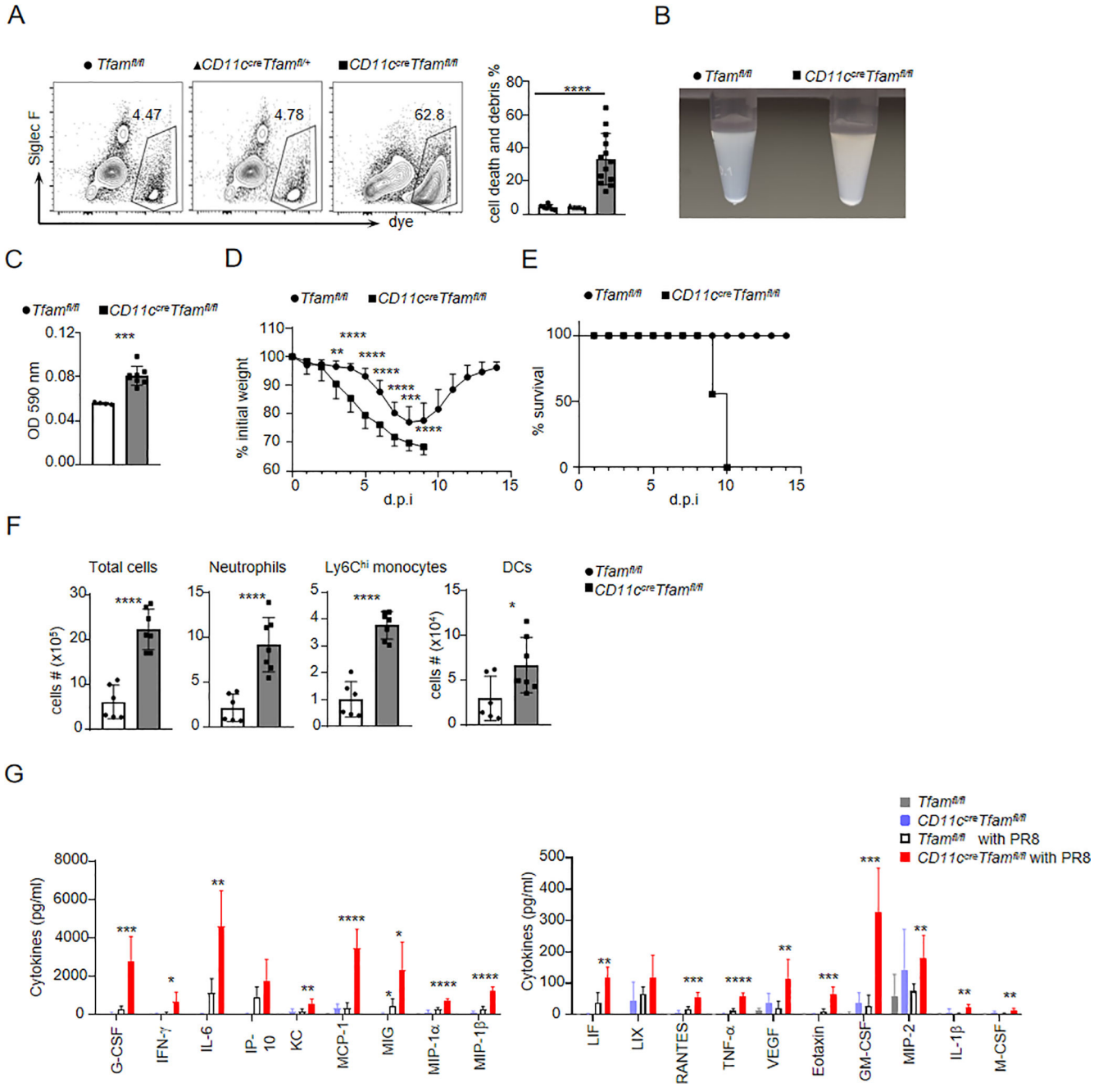

FIGURE 5. TFAM deficiency increases host susceptibility to severe influenza virus infection.

(**A**) Flow cytometry analysis of cell death and debris in naïve BAL from *Tfam*$^{fl/fl}$, *CD11c*^{cre}*Tfam*$^{fl/+}$ and *CD11c*^{cre}*Tfam*$^{fl/fl}$ mice at the age of 7–8 weeks. (**B** and **C**) The representative images (B) and value of OD590 (C) of naïve BAL fluid from *Tfam*$^{fl/fl}$, and *CD11c*^{cre}*Tfam*$^{fl/fl}$ mice at the age of 7–8 weeks. (D-G) *Tfam*$^{fl/fl}$ and *CD11c*^{cre}*Tfam*$^{fl/fl}$ mice were infected with influenza virus. (**D** and **E**) The body weight loss (D) and survival (E) of *CD11c*^{cre}*Tfam*$^{fl/fl}$ mice in response to virus infection compared with *Tfam*$^{fl/fl}$ mice, n = 10, 9. (**F**) The cell numbers of total cells and innate cells including neutrophils, Ly6C^{hi} monocytes and DCs in BAL at 4 d.p.i, n = 6, 7. (**G**) BAL concentrations of cytokines and

chemokines in indicated mouse strains with or without influenza infection (4 d.p.i.). Data are presented as arithmetic means ± SD. *, $p < 0.05$; **, $p < 0.01$; ***, $p < 0.001$.

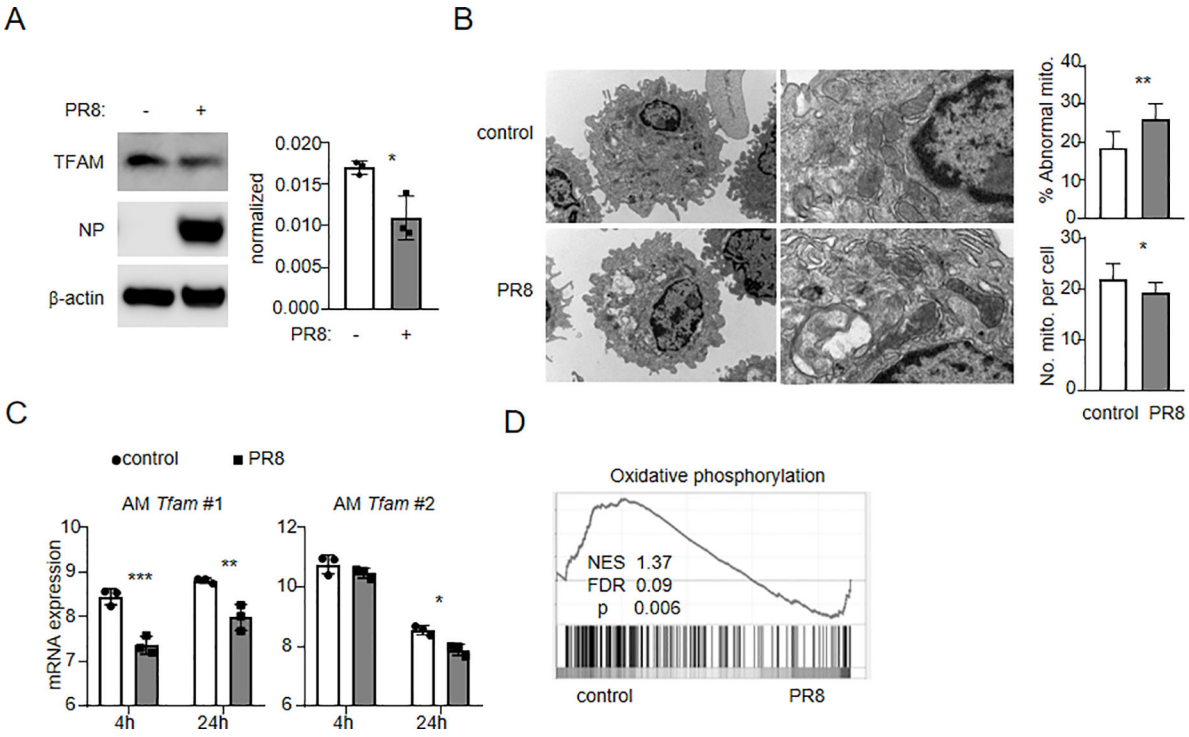

FIGURE 6. Influenza virus infection diminishes TFAM expression and causes AM mitochondrial damage.

(**A**) Western blot analysis for TFAM expression in AMs with or without PR8 infection for 24 h. Representative blots and quantification were from three independent experiments. (**B**) Transmission electron microscopy images of AMs with or without PR8 infection for 24 h *in vitro*. Scale bars, 5μm (left panel) or 1μm (right panel). Quantification of mitochondrial numbers and percentages of abnormal mitochondria in AM are shown on the right. (**C**) The mRNA levels of transcript variant 1 and 2 of *Tfam* gene in human AMs with or without PR8 infection for 4 h or 24 h in publicly available microarray dataset (GSE30723). (**D**) Publicly available microarray dataset of human AMs (obtained from 3 patients) that were infected with PR8 for 24 h *in vitro* (GSE30723). Enrichment plot from GSEA of human AMs using gene sets for Oxidative phosphorylation were shown. Data are presented as arithmetic means ± SD. *, $p < 0.05$; **, $p < 0.01$; ***, $p < 0.001$.